



**HAL**  
open science

## **SALOMON: a new, light balloonborne UV-visible spectrometer for nighttime observations of stratospheric trace-gas species**

Jean-Baptiste Renard, Michel Chartier, Claude Robert, Gilles Chalumeau, Gwenaël Berthet, Michel Pirre, Jean-Pierre Pommereau, Florence Goutail

### ► To cite this version:

Jean-Baptiste Renard, Michel Chartier, Claude Robert, Gilles Chalumeau, Gwenaël Berthet, et al.. SALOMON: a new, light balloonborne UV-visible spectrometer for nighttime observations of stratospheric trace-gas species. *Applied optics*, 2000, 39 (3), pp.386-392. 10.1364/AO.39.000386. insu-02879192

**HAL Id: insu-02879192**

**<https://insu.hal.science/insu-02879192v1>**

Submitted on 25 Feb 2024

**HAL** is a multi-disciplinary open access archive for the deposit and dissemination of scientific research documents, whether they are published or not. The documents may come from teaching and research institutions in France or abroad, or from public or private research centers.

L'archive ouverte pluridisciplinaire **HAL**, est destinée au dépôt et à la diffusion de documents scientifiques de niveau recherche, publiés ou non, émanant des établissements d'enseignement et de recherche français ou étrangers, des laboratoires publics ou privés.

# SALOMON: a new, light balloonborne UV-visible spectrometer for nighttime observations of stratospheric trace-gas species

Jean-Baptiste Renard, Michel Chartier, Claude Robert, Gilles Chalumeau, Gwenaël Berthet, Michel Pirre, Jean-Pierre Pommereau, and Florence Goutail

A new, light balloonborne UV-visible spectrometer, called SALOMON, is designed to perform nighttime measurements of stratospheric trace-gas species by using the Moon as a light source. The first flight, performed on 31 October 1998 at mid-latitude with a float altitude of 26.7 km, allowed the performance of the pointing system to be checked and vertical profiles of ozone, NO<sub>2</sub>, NO<sub>3</sub>, and possibly OBrO to be obtained. First the instrument and then the performance of the pointing system and the detector are described. Finally the vertical profiles are compared with other profiles obtained at the same location five years before with the heavier balloonborne spectrometer AMON, which uses a star as the light source.

## 1. Introduction

NO<sub>2</sub>, NO<sub>3</sub>, and OClO are involved in stratospheric ozone chemistry. These gas-phase species, as well as ozone, possess some absorption bands that are detectable in the near-UV-visible spectral domain. The extinction coefficient of aerosol can also be measured because it presents a strong UV-visible continuum below 25 km. At the present time, several balloonborne UV-visible spectrometers that use the Sun as a light source are in operation, but only one balloonborne UV-visible spectrometer, AMON (French acronym for Absorption par les Minoritaires Ozone et NO<sub>x</sub>),<sup>1,2</sup> takes measurements at night, using a star as the light source. AMON, aboard the stabilized platform of the Geneva Observatory,<sup>3</sup> which has a pointing system accuracy of 3 arc sec, can achieve a vertical resolution of less than 1 km. Because it has a total weight of 500 kg, AMON must be launched with a balloon whose

volume gas capacity is at least 100,000 m<sup>3</sup>. This requirement implies constraints that reduce the launch opportunities.

Recent studies have shown that, despite good agreement between modeling results and observations of OClO at high latitudes,<sup>4,5</sup> significant discrepancies exist for NO<sub>2</sub> and NO<sub>3</sub> at mid-latitude and high latitude.<sup>2,6,7</sup> Moreover, the possible detection of OBrO by the AMON,<sup>8</sup> although models predict no OBrO at all,<sup>9</sup> as well as the possible observation of BrO at night in the polar vortex<sup>10</sup> could imply that bromine chemistry is not well understood. All these facts call for many other nighttime observations at different seasons, latitudes, and local times to improve the database for these species. To perform such measurements, a light instrument with reduced launch constraints is needed.

The light of a star is weak and requires an accurate and heavy pointing system. The Moon, which needs a less accurate pointing system, can be used as a light source to reduce the weight of the instrument. This method of measurement has been already used for ground-based and airborne spectrometers (see, e.g., Sanders *et al.*<sup>11</sup> and Lal *et al.*<sup>12</sup>) but not by balloonborne instruments.

A new instrument, called SALOMON (which is a French acronym for Spectroscopie d’Absorption Lunaire pour l’Observation des Minoritaires Ozone et NO<sub>x</sub>), funded by the French space agency Centre National d’Etudes Spatiales (CNES), is now operating.

---

J.-B. Renard (jbrenard@cncs-orleans.fr), M. Chartier, C. Robert, G. Chalumeau, G. Berthet, and M. Pirre are with the Laboratoire de Physique et Chimie de l’Environnement, Centre National de la Recherche Scientifique, 45071 Orleans Cedex 2, France. J.-P. Pommereau and F. Goutail are with the Service d’Aéronomie du Centre National de la Recherche Scientifique, BP3, 91371 Verrières le Buisson cedex, France.

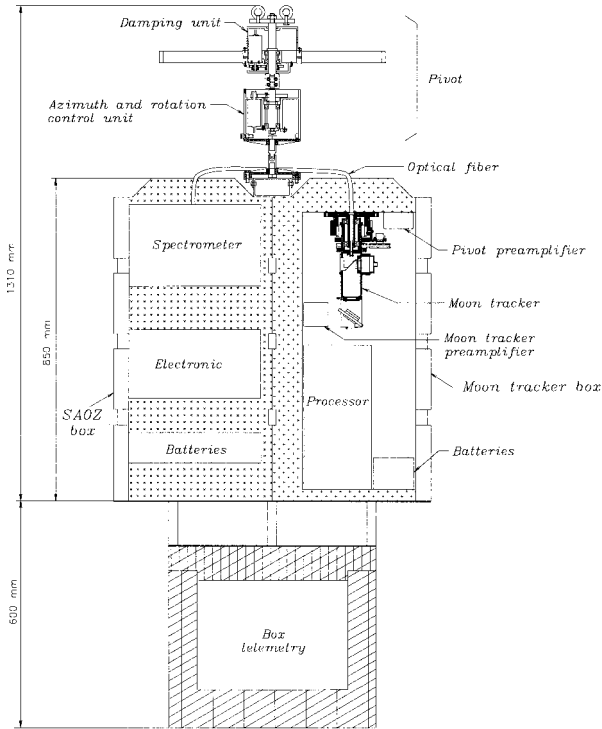


Fig. 1. Global view of the SALOMON. The box that contains the spectrometer is at the left, the box with the moon tracker is at the right, and the box with the CNES telemetry is below them.

It was developed based on the experience acquired by the AMON team and by the team that developed the light balloonborne UV–visible spectrometer SAOZ<sup>13</sup> that uses the Sun as a light source. SALOMON was first flown successfully on 31 October 1998 at mid-latitude.

We present below a description of this instrument and the first results, including performance of the pointing system, spectra, and vertical profiles of the species.

## 2. Description of the Instrument

### A. General Description

SALOMON is made from three boxes (Fig. 1). The top two boxes, linked by an optical fiber, include a spectrometer and the moon-tracker system. The third, below the two others, contains the CNES telemetry system. The boxes are made from polystyrene, which is well suited for protecting the onboard instruments at landing. The pivot (i.e., the primary pointing system) is located above the boxes and links the gondola to the flight chain (which includes a Global Positioning System, a barometer, and the parachutes) and the balloon. The total weight of SALOMON is 80 kg, which permits the use of balloons in the 10,000–65,000-m<sup>3</sup> range to reach a float altitude of 18–3 hPa (i.e., 27–38 km at mid-latitudes). This instrument operates automatically for on–off switching, pointing, data acquisition, and telemetry.

The housekeeping and spectroscopic data are telemetered in real time to the ground.

The measurements are performed by the lunar occultation method. This method consists of recording spectra affected by atmospheric absorption during a moonset or a moonrise. The elevation of the Moon decreases from a few degrees above the gondola’s horizon to  $\sim -4^\circ$ , which implies a duration at float of  $\sim 40$  min. A reference spectrum is recorded when the Moon is as high as possible and the balloon is at float. In fact, observations performed using the Sun or stars have shown that the reference spectrum is only slightly affected by atmospheric species when the light source is more than  $2^\circ$  above the gondola’s horizon. In that case, the contribution of the species to the reference spectrum is less than 5% of the maximum contribution of the species to the occultation spectra. We then obtain transmission spectra by dividing the Moon’s occultation spectra by the reference spectrum. Finally, we obtain the optical depth spectra that are used to retrieve slant column densities of atmospheric species along the line of sight by taking the opposite of the logarithm of the transmission spectra.

### B. The Pivot

The pivot (or stabilization unit) is designed to stabilize the gondola and to perform rough azimuth control. It is composed of a magnetic damping device to stabilize the flight chain and a mechanical unit with a velocity sensor to perform the gondola rotation. The motor (RE35G-071-34, built by Mascon) is driven by a numerical control feedback for the gondola’s rotation and an analog control feedback for the gondola’s azimuth stabilization. The Moon’s location in the sky is determined automatically by two photodiodes mounted  $45^\circ$  from each other. The pivot induces a rotation of the gondola until the fluxes on the two photodiodes are identical. This system is designed to have a precision of less than  $0.2^\circ$ , which is less than half of the Moon’s diameter, and to operate when the light flux is greater than 15% of the full Moon’s global flux (i.e., between its first quarter and last quarter).

### C. The Moon Tracker

The moon tracker (Fig. 2) consists of a 25 mm  $\times$  76 mm plane mirror that can move on elevation (motor BTN 18-D, built by Vernitron), mounted upon a turret that turns on azimuth (motor 3181V-12I-053, built by Vernitron). A portion of the light focused by a lens in the turret is sent to a position sensor, which determines the spot ( $x, y$ ) position. The error in elevation and the error in azimuth are calculated, and the calculated correction is sent directly to the motors by the onboard processor. The system is designed to achieve a precision below 30 arc sec when the gondola is affected by only small perturbations. In the case of strong oscillations of the gondola, as can be encountered during ascent of the balloon, the error on azimuth can be as much as 1 arc min, and the error

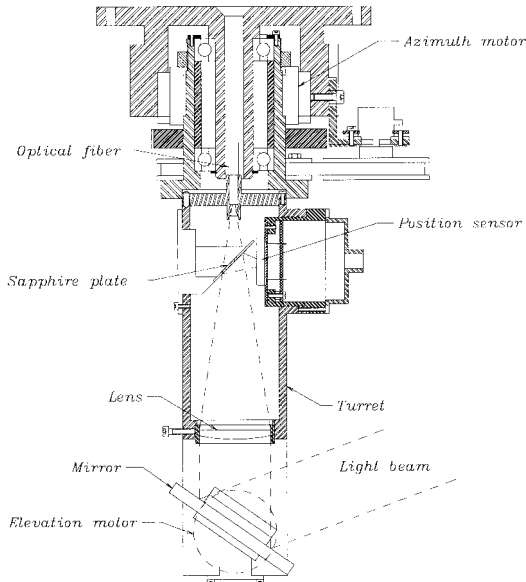


Fig. 2. Schematic diagram of the moon tracker.

on elevation can reach a few arc minutes because this axis is not controlled by the pivot.

The flux collected by the mirror is focused onto an optical fiber to send the light to the spectrometer. This device homogenizes the flux and eliminates sensitivity to the variations of the Moon's albedo induced by its nonuniform ground composition.

#### D. The Spectrometer

The spectrometer, the detector, and the electronics are the same as those used for the SAOZ instrument,<sup>13</sup> which had performed 80 flights by the end of 1998. The spectrometer is a Jobin-Yvon Model CP200, with a wavelength domain shifted to 350–700 nm to cover the  $\text{NO}_3$  absorption band at 662 nm. The detector is a Hamamatsu photodiode array of 1024 pixels, with a theoretical spectral resolution of 0.34 nm, which is 2.5 times the theoretical resolution of AMON. For the first flight, an entrance slit of 100  $\mu\text{m}$  was used to maximize the flux. The exposure time was 52 s, which is suitable for producing a high signal-to-noise ratio without degrading the expected 2-km vertical resolution. A dark current exposure is performed after every ten exposures, and its value is subtracted automatically from the recorded spectra by the onboard processor.

### 3. Results of the First Flight

#### A. Flight Conditions

The first flight of SALOMON occurred during the night of 30–31 October 1998 from the CNES launching base of Aire sur l'Adour, France (43.7 N, 0.3 W). This flight was devoted to testing all the technical parameters of the instrument, and a 12,000- $\text{m}^3$  balloon was used. Flight conditions allowed for measurements to be performed during the ascent of the balloon and during the whole moonset. Inasmuch

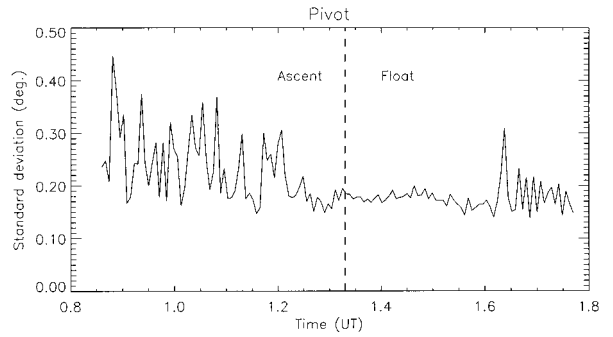


Fig. 3. Pointing precision of the pivot.

as all the parameters of the pointing system, the moon tracker, and the spectrometer were nominal, scientific results can be extracted from the spectra.

Launch occurred at 00:06 UT, the ascent lasted 75 min, and the float altitude of the balloon was 26.65 km (19 hPa) with fluctuations of  $\pm 150$  m. This altitude is suitable for the observation of  $\text{O}_3$  but is problematic for observation of  $\text{NO}_2$  and  $\text{NO}_3$  because the maximum concentrations of these species are above 27 km. Corrections are then needed, as described below in Subsection 3.C. The measurements started at 00:52 UT, just after crossing the tropopause, and stopped at 01:46; 43 spectra were recorded. Because of strong winds and the fast ascent of the balloon, some oscillations of the gondola occurred during the observations and stopped only a few minutes before the end of the measurements at float altitude. Without affecting the spectra, this situation allowed for testing of the pointing system both in perturbed and in quiet conditions.

The phase of the Moon was 68% of full. Inasmuch as the flux was strong enough for both the spectrometer and the pointing system, this flight demonstrated that measurements can be performed less than two days after the first quarter. Thus flights can occur at least 10 days per month, not including the day of the full Moon for which moonrise and moonset occur too close to sunset and sunrise.

#### B. Performance of the Instrument

Figures 3, 4, and 5 show the pointing precision of the pivot, the moon-tracker azimuth, and the moon-

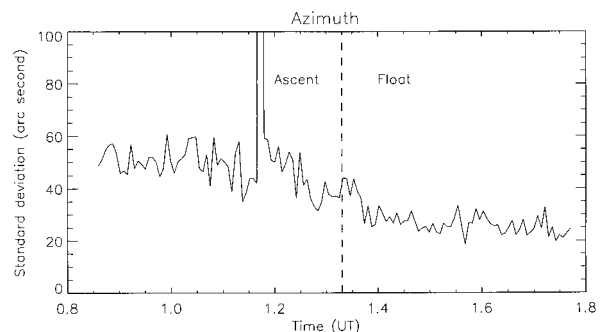


Fig. 4. Pointing precision of the azimuth of the moon tracker.

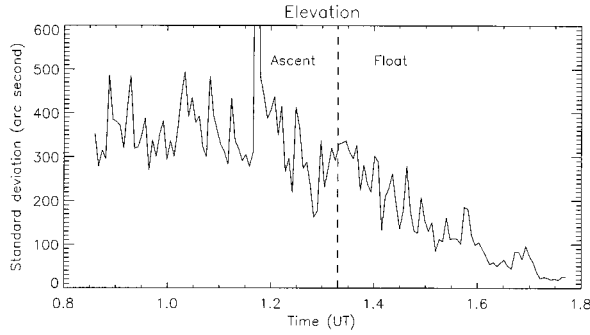


Fig. 5. Pointing precision of the elevation of the moon tracker.

tracker elevation, respectively. The pivot reached its expected precision, i.e., below  $0.2^\circ$ . The precision of the moon-tracker azimuth was close to 1 arc min during the ascent of the balloon and reached the expected 30 arc sec at float. The precision of the moon-tracker elevation was of a few arc minutes during the ascent, decreased to 1 arc min at float, but remained above the expected 30 arc sec because of the gondola movements. During the last 10 min at float, these movements stopped, and the expected value was reached.

The analysis of the position of the Moon's Ca, H, and Na absorption lines in all the spectra shows that the wavelength shift from the first spectrum to the last spectrum is less than 0.03 pixel (i.e., 0.01 nm). This value is close to the theoretical shift induced by the variation of air density and its refractive index. Thus the spectra recorded during the Moon's occultation can be divided by the reference spectrum without shift adjustment, which prevents the appearance of artificial absorption features. The noise is found to be equal to 3.8 digital levels, whereas the signal is close to 10,000 digital levels. Thus a signal-to-noise ratio greater than 2500 per pixel is obtained.

### C. Data Reduction and Results

The Moon occultation method requires highly accurate Moon coordinates to enable the inversion be performed and the minimum altitude of each line of sight to be known. The Moon's elevation and azimuth were calculated with the exact location and altitude of the balloon taken into account. The topocentric Moon coordinates were calculated by use of the Bureau des Longitudes on-line data.<sup>14</sup>

Figure 6 presents the raw spectra recorded during the occultation. The cosmic rays, which affect only a few pixels per spectrum, were removed by use of the algorithm previously developed for AMON.<sup>1</sup> The reference spectrum is the result of averaging five consecutive spectra recorded with a Moon elevation of  $2.5^\circ$  to  $1.5^\circ$ . The algorithms used for data reduction of the transmission spectra are similar to those used for AMON, which are described in detail by Renard *et al.*<sup>2,8</sup> The wavelength scale was established from the lunar Ca (K), Ca (H), H $\delta$ , Fe(d), H $\beta$ , Na, H $\alpha$ , and atmospheric O<sub>2</sub> lines and a second-order polynomial fit (with a standard deviation smaller than 0.05 nm).

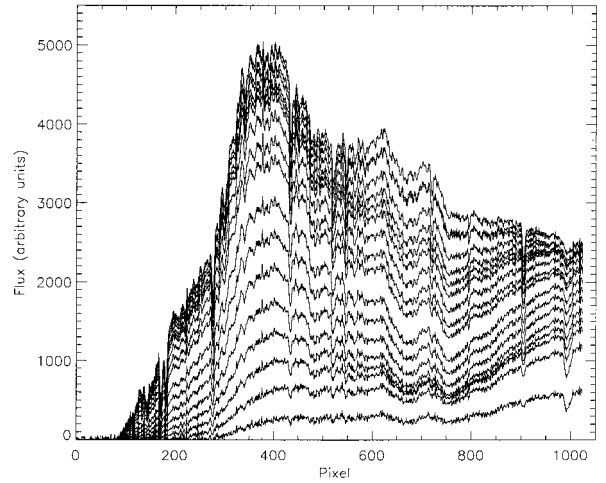


Fig. 6. Raw spectra recorded during the occultation (cosmic rays have been removed).

Because of the weakness of the Moon's flux in the UV, the spectral domain was reduced to 400–700 nm. The Rayleigh scattering contribution, calculated by use of the cross sections given by Bucholtz,<sup>15</sup> was removed from all spectra. The complete coverage of the visible spectral domain allows O<sub>3</sub> and NO<sub>2</sub> absorption features to be used over large spectral ranges of 455–680 and 400–550 nm, respectively. Ozone retrieval was performed with the aerosol contribution that follows a second-order polynomial law taken into account. The NO<sub>2</sub> retrieval was performed by use of a differential method with a high-pass filter to remove the continuum. With respect to NO<sub>3</sub>, the analysis performed on AMON data has shown that the spectral domain must be restricted to 645–680 nm to avoid inclusion of an oxygen line close to the NO<sub>3</sub> 623-nm band.

Figure 7 presents an example of the recorded optical depth spectrum, smoothed over 6 pixels, recorded with a Moon elevation of  $-1.0^\circ$ , and the O<sub>3</sub> least-squares fit with the cross section at 223 K measured at Bremen University.<sup>16</sup> Figures 8 and 9 present the NO<sub>2</sub> and the NO<sub>3</sub> retrieval for the same spectrum, smoothed over 5 and 6 pixels, respectively. The NO<sub>2</sub> cross sections used were measured by

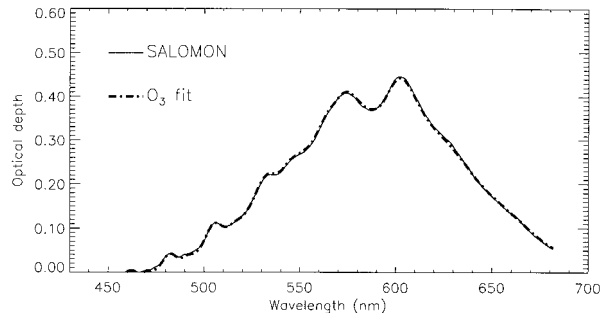


Fig. 7. Comparison of an O<sub>3</sub> optical depth spectrum recorded by the SALOMON, with a moon elevation of  $-1.0^\circ$ , and a least-squares fit.



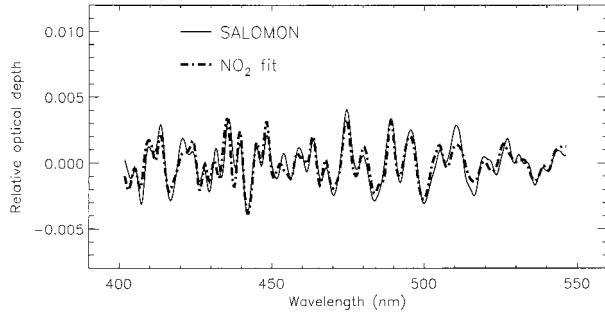


Fig. 8. Comparison of a  $\text{NO}_2$  optical depth spectrum recorded under the same conditions as for Fig. 7 and a least-squares fit.

Harder *et al.*<sup>17</sup> at 217 K, and the  $\text{NO}_3$  cross sections used were measured at 243 K by Deters and Burrows.<sup>18</sup> The error that results from calculations of the standard deviation between the fit and the observed optical depth spectrum is  $3 \times 10^{-3}$ ,  $6 \times 10^{-4}$ , and  $3 \times 10^{-3}$  for  $\text{O}_3$ ,  $\text{NO}_2$ , and  $\text{NO}_3$  respectively. Finally, we can obtain the aerosol extinction coefficient by subtracting the contribution of all the species described above.

Figure 10 shows the slant column profiles versus Moon elevation for  $\text{O}_3$ ,  $\text{NO}_2$ ,  $\text{NO}_3$ , and aerosols at blue and red wavelengths. Because the measurements were made at the low float altitude of 26.5 km, the contribution of the species to the reference spectrum cannot be neglected; negative values therefore appear for observations performed during the balloon ascent when the Moon elevation was between  $6^\circ$  and  $2^\circ$ . Performing the inversion to obtain concentrations requires that the slant column profile be corrected by the offset contained in the reference spectrum. The first value of the slant column density profile for each species provides an estimation of this offset, or at least of its lower limit. These values will then be added to the slant column profiles.

#### 4. Comparison with the AMON Instrument

As we discussed in Section 1, only one instrument, AMON, has performed measurements by UV-visible spectrometry at night. The performance of the AMON pointing system is greater than that of the SALOMON pointing system, as stellar observations

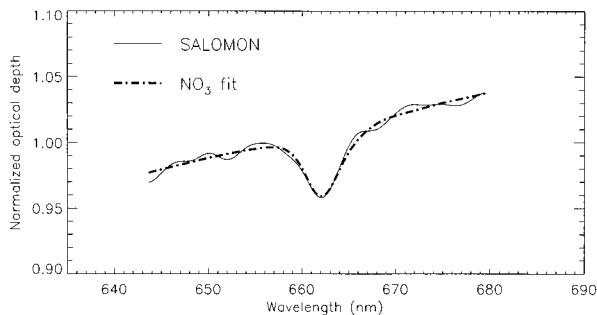


Fig. 9. Comparison of a  $\text{NO}_3$  optical depth spectrum recorded under the same conditions as for Fig. 7 and a least-squares fit.

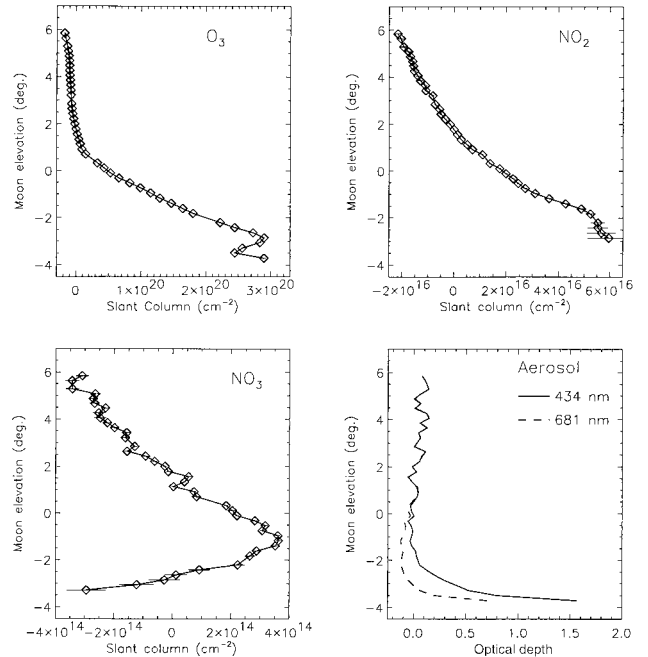


Fig. 10. Slant column profiles of  $\text{O}_3$ ,  $\text{NO}_2$ ,  $\text{NO}_3$ , and aerosol (at two wavelengths). The negative values originate from the contributions of these species to the reference spectrum.

need greater accuracy (the angular diameter of a star is below 1 arc sec, whereas that of the Moon it is 30 arc min). Nevertheless, the performance of SALOMON is well suited for Moon observations, as discussed above.

The  $\text{O}_3$  and  $\text{NO}_2$  retrieval is performed over a larger spectral domain with SALOMON than with AMON: 225 versus 75 nm for  $\text{O}_3$  and 150 versus 60 nm for  $\text{NO}_2$ . These larger spectral domains ensure that no error exists on the SALOMON wavelength scale, which is essential for the retrieval of small absorption features.

Inasmuch as the Moon flux is greater than the star flux, and because no wavelength shift was detected, one would expect that the SALOMON spectrometer can detect smaller absorption features than the AMON can. This flight showed that  $\text{NO}_2$  and  $\text{NO}_3$  are detected by the SALOMON with a greater signal-to-noise ratio, and therefore sensitivity, than with the AMON (sensitivity of  $5 \times 10^{-4}$  for the SALOMON compared with  $5 \times 10^{-3}$  for the AMON in the case of  $\text{NO}_2$  and  $\text{NO}_3$  detection). This fact allowed us to search for OBrO in the SALOMON spectra. The retrieval of OBrO was performed by the method described by Renard *et al.*<sup>8</sup> and with the new cross sections measured at 298 K by Fleischmann *et al.*<sup>19</sup> Because the  $\text{NO}_2$  cross sections of Harder *et al.*<sup>17</sup> stop at 550 nm, and the OBrO cross sections before 470 nm are below our detection limit, the spectral domain for the retrieval is just slightly greater than in the AMON retrieval. A sliding average was performed over three consecutive spectra for lines of sight above 24 km and five consecutive spectra below 24 km to reduce the noise; then the spectra were smoothed over 9 pixels.

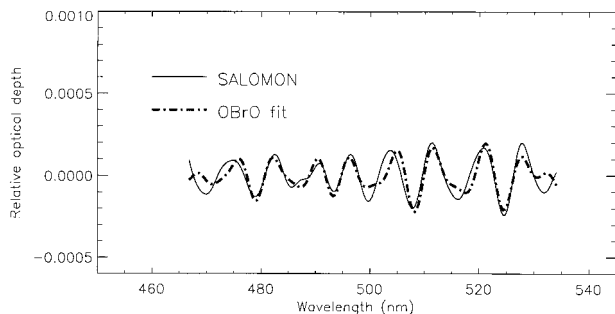


Fig. 11. Comparison of an OBrO optical depth spectrum recorded under the same conditions as in Fig. 7 and a least-squares fit.

Figure 11 shows a comparison between a SALOMON spectrum and a fit from the OBrO cross sections. The error, corresponding to the standard deviation between fit and observed spectrum, is equal to  $5 \times 10^{-5}$ , which is close to the theoretical limit of the instrument when the smoothing procedures described above are taken into account. This result shows that the SALOMON can detect absorption features of  $10^{-4}$ , which is a slightly better sensitivity than that of ground-based and airborne lunar occultation instruments<sup>11,12</sup> and ten times better than that of AMON, and that the OBrO detection by AMON does not come from instrumental bias.

Figure 12 presents the vertical profiles of these species, after their inversion by an onion-peeling algorithm, and a comparison of them with AMON vertical profiles obtained at the same location on 16 October 1993 (the AMON profile retrievals had been

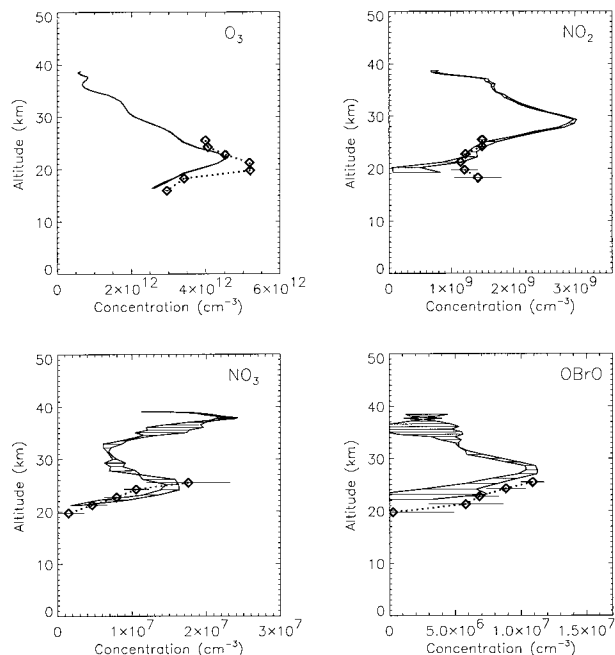


Fig. 12. Vertical profiles of  $O_3$ ,  $NO_2$ ,  $NO_3$ , and OBrO measured by the SALOMON (diamonds) compared with the AMON measurements (solid curves) performed at the same location on 16 October 1993.

improved since the papers of Renard *et al.*<sup>2,8</sup> were published). As the AMON flight was performed at a float altitude of 39 km, the AMON profiles cover a larger altitude range in the stratosphere than the SALOMON profiles. Nevertheless, the shapes of the two sets of profiles are in good agreement, and the small discrepancies result from different geophysical conditions during the two measurements. Thus these SALOMON observations will be included in the database for further studies of nitrogen species at night by comparison with modeling outputs.

## 5. Conclusion

The first flight of SALOMON has shown that the performance of the instrument is as good as expected. Only small modifications (the use of optical fiber and lenses with better transmission) will be made for the next flights. Thus the global flux on the detector will be increased so the OCIO absorption features from 380 to 425 nm can be detected for flights at high latitudes.

As SALOMON can be prepared for launch in only a few days, can be launched in windy conditions (as much as  $5 \text{ m s}^{-1}$  at ground), and can operate over a wide range of float altitudes, several flights per year can be performed with various scientific objectives. Currently, two flights are planned for the Third European Stratospheric Experiment on Ozone (THESEO) campaign for the nighttime study of  $NO_2$  and  $NO_3$ , and moonrise measurements will be tried for the second flight. A few flights are planned for years 2000 and 2001, in particular during validation campaigns of instruments onboard such satellite platforms as SAGE III, ILAS/ADEOS, GOMOS/ENVISAT, and SCIAMACHY/ENVISAT. This instrument may also be involved in the study of the tropics by European groups of scientists that could occur beginning in 2003.

We thank all the persons in our laboratories, in particular Pierre François, who have contributed to the successful performance of this instrument. We also thank the CNES for funding the instrument, and the CNES launching team at Aire sur l'Adour.

## References and Notes

1. J. P. Naudet, C. Robert, and D. Hugué, "Balloon measurements of stratospheric trace species using a multichannel UV-visible spectrometer," in *Proceedings of the 14th ESA Symposium on European Rocket and Balloon Programs and Related Research* (European Space Agency, Paris, 1994), pp. 165–168.
2. J. B. Renard, M. Pirre, C. Robert, G. Moreau, D. Hugué, and J. M. Russell III, "Nocturnal vertical distribution of stratospheric  $O_3$ ,  $NO_2$  and  $NO_3$  from balloon measurements," *J. Geophys. Res.* **101**, 28,793–28,804 (1996).
3. D. Hugué, "Design and performance of stratospheric balloon-borne platforms for infrared astrophysical observations," *Infrared Phys. Technol.* **35**, 195–202 (1994).
4. J. P. Pommereau and J. Piquard, "Observations of the vertical distribution of stratospheric OCIO," *Geophys. Res. Lett.* **21**, 1231–1234 (1994).

5. J. B. Renard, F. Lefèvre, M. Pirre, C. Robert, and D. Huguenin, "Vertical profile of night-time stratospheric OCIO," *J. Atmos. Chem.* **26**, 65–76 (1997).
6. D. J. Lary, R. Toumi, A. M. Lee, M. Newchurch, M. Pirre, and J. B. Renard, "Carbon aerosols and atmospheric photochemistry," *J. Geophys. Res.* **102**, 3671–3682 (1997).
7. J. B. Renard, M. Pirre, F. Lefevre, C. Robert, B. Nozière, E. Lateltin, and D. Huguenin, "Vertical distribution of nighttime stratospheric NO<sub>2</sub> from balloon measurements—comparison with models," *Geophys. Res. Lett.* **24**, 73–76 (1997).
8. J. B. Renard, M. Pirre, C. Robert, and D. Huguenin, "The possible detection of OBrO in the stratosphere," *J. Geophys. Res.* **103**, 25,383–25,395 (1998).
9. M. P. Chipperfield, T. Glassup, I. Pundt, and O. V. Rattigan, "Model calculations of stratospheric OBrO indicating very small abundances," *Geophys. Res. Lett.* **25**, 3575–3578 (1998).
10. A. Wahner, J. Callies, H. P. Dorn, U. Platt, and C. Schiller, "Near UV atmospheric absorption measurements of column abundance during airborne arctic expedition, January–February 1989. 3. BrO observations," *Geophys. Res. Lett.* **17**, 517–520 (1990).
11. R. W. Sanders, S. Solomon, M. A. Carroll, and A. L. Schmeltekopf, "Visible and near-ultraviolet spectroscopy at McMurdo Station, Antarctica. 4. Overview and daily measurements of NO<sub>2</sub>, O<sub>3</sub> and OCIO during 1987," *J. Geophys. Res.* **94**, 11,381–11,391 (1989).
12. M. Lal, J. S. Sidhu, S. R. Das, and D. K. Chakrabarty, "Atmospheric NO<sub>3</sub> observations over low-latitude northern hemisphere during night," *J. Geophys. Res.* **98**, 23,029–23,037 (1993).
13. J. P. Pommereau and J. Piquard, "Ozone, nitrogen dioxide and aerosol vertical distribution by UV–visible solar occultation from balloon," *Geophys. Res. Lett.* **21**, 1227–1230 (1994).
14. On-line data available at the internet site of the Bureau des Longitudes, [www.bdl.fr](http://www.bdl.fr).
15. A. Bucholtz, "Rayleigh-scattering calculations for the terrestrial atmosphere," *Appl. Opt.* **34**, 2765–2773 (1995).
16. S. Voigt, J. Orphal, and J. P. Burrows, information available at their internet site, [www.iup.physik.uni-bremen.de/gruppen/data.html](http://www.iup.physik.uni-bremen.de/gruppen/data.html).
17. J. W. Harder, J. W. Brault, P. V. Johnston, and G. H. Mount, "Temperature dependent NO<sub>2</sub> cross sections at high spectral resolution," *J. Geophys. Res.* **102**, 3861–3879 (1997).
18. B. Deters and J. P. Burrows, Institute of Environmental Physics and Remote Sensing, IUP/IFE, University of Bremen-FB1, Postfach 30440, 28334 Bremen, Germany (personal communication, 1998).
19. O. C. Fleischmann, M. Hartmann, and J. P. Burrows, Institute of Environmental Physics and Remote Sensing, IUP/IFE, University of Bremen-FB1, Postfach 30440, 28334 Bremen, Germany (personal communication, 1998).